Astron. Astrophys. 336, L57–L60 (1998)

ASTRONOMY AND ASTROPHYSICS

LETTER

Letter to the Editor

The prolate solar chromosphere

F. Auchère[1], S. Boulade[2], S. Koutchmy[2], R.N. Smartt[3], J.P. Delaboudinière[1], A. Georgakilas[4], J.B. Gurman[5], and G.E. Artzner[1]

[1] Institut d'Astrophysique Spatiale, Bâtiment 121, Université Paris XI, F-91405 Orsay Cedex, France
[2] Institut d'Astrophysique de Paris, 98 bis Boulevard Arago, F-75014 Paris, France
[3] NSO/Sacramento Peak Observatory, Sunspot, NM 88349, USA
[4] National Observatory, Athens, Greece
[5] NASA/Goddard Space Flight Center, Greenbelt, MD, USA

Received 27 April 1998 / Accepted 18 June 1998

Abstract. We present a comparative analysis of the chromospheric solar limb prolateness, using strictly simultaneous H_α ground-based observations and HeII space-based observations. The typical prolateness is found to be $\Delta D/D = 5.5 \times 10^{-3}$ in HeII and 1.2×10^{-3} in H_α. The first measurements in the 30.4 nm HeII line over a period of two years, as well as coronal data, are discussed to explore further the origin of the prolateness and its possible consequences.

Key words: Sun: chromosphere – corona

1. Introduction

Since the earliest space observations, it has been known that the radial gradient for many TR lines, including the HeII lines, is lower inside coronal holes than outside (Withbroe et al., 1976 or Huber et al., 1974). From historic visual H_α observations, it was evident that the polar chromosphere looks more extended than the low latitude chromosphere (Secchi, 1877). More recent measurements confirmed that characteristic (Beckers, 1960 or Dunn, 1960). At the same time, the theoretically expected oblate shape of the Sun (oblateness or flattening) at photospheric levels was measured repeatedly by many observers. Today, those older observations have been surperseded by modern measurements (Rozelot & Rösch, 1996 or Kuhn et al., 1997) that reduced this eventual oblatness to a small, but finite, value of order of 10^{-2} arcsec. Accordingly, the shape of the Sun at the chromospheric levels needs further investigation. Although theoretically unexpected, we present here the first quantitative measurements of the prolate shape of the chromosphere as simultaneously measured in H_α and in the HeII line at 30.4 nm. We also present statistically more significant values derived for both the high chromosphere and the very inner corona.

Send offprint requests to: F. Auchère

2. Results of the August 1997 observing campaign

2.1. Limb features

During a recent observing run at the NSO/Sacramento Peak Vacuum Tower Telescope (VTT), data obtained in H_α, and in other lines, were compared with those from the Extreme-Ultraviolet Imaging Telescope (EIT) onboard SoHO recorded in the intermediate temperature range ($T \sim 6.10^4$) HeII line at 30.4 nm. As had been already suggested more than two decades earlier from unique UBF H_α data taken at the Sacramento Peak VTT and from quasi-simultaneous HeII photographic data from Skylab (Moe et al., 1974), it was confirmed that there is little apparent correspondence between spicule-like features seen over corresponding sections of the solar limb in the two lines, especially so in the polar regions near sunspot minimum. While any one prominence "system" can appear in both images, frequently it is visible only in the HeII image. And the detailed structures are usually quite different (Delannee et al., 1997). Understanding the relationship between such radically different views of the solar atmosphere is an area of major current interest in solar physics.

2.2. The overall limb

The HeII data were also compared with simultaneously recorded H_α limb data from the NSO/SP 20-cm aperture emission-line coronagraph, both types of images covering the full limb (see Fig. 1). Coronograph full limb H_α images show significantly more extended features than those from the VTT, since the level of scattered light is much lower in the coronograph as compared with the VTT, and a broader filter is used. Moreover the instrumental distorsion is completly negligible at the 0.1 arcsecond level because the whole instrument, as with any classical coronograph, is strictly on-axis and the whole image is recorded simultaneously. The HeII images were processed with an occulting mask to simulate the form of the coronagraph images, and a cross-correlation method involving small azimuthal

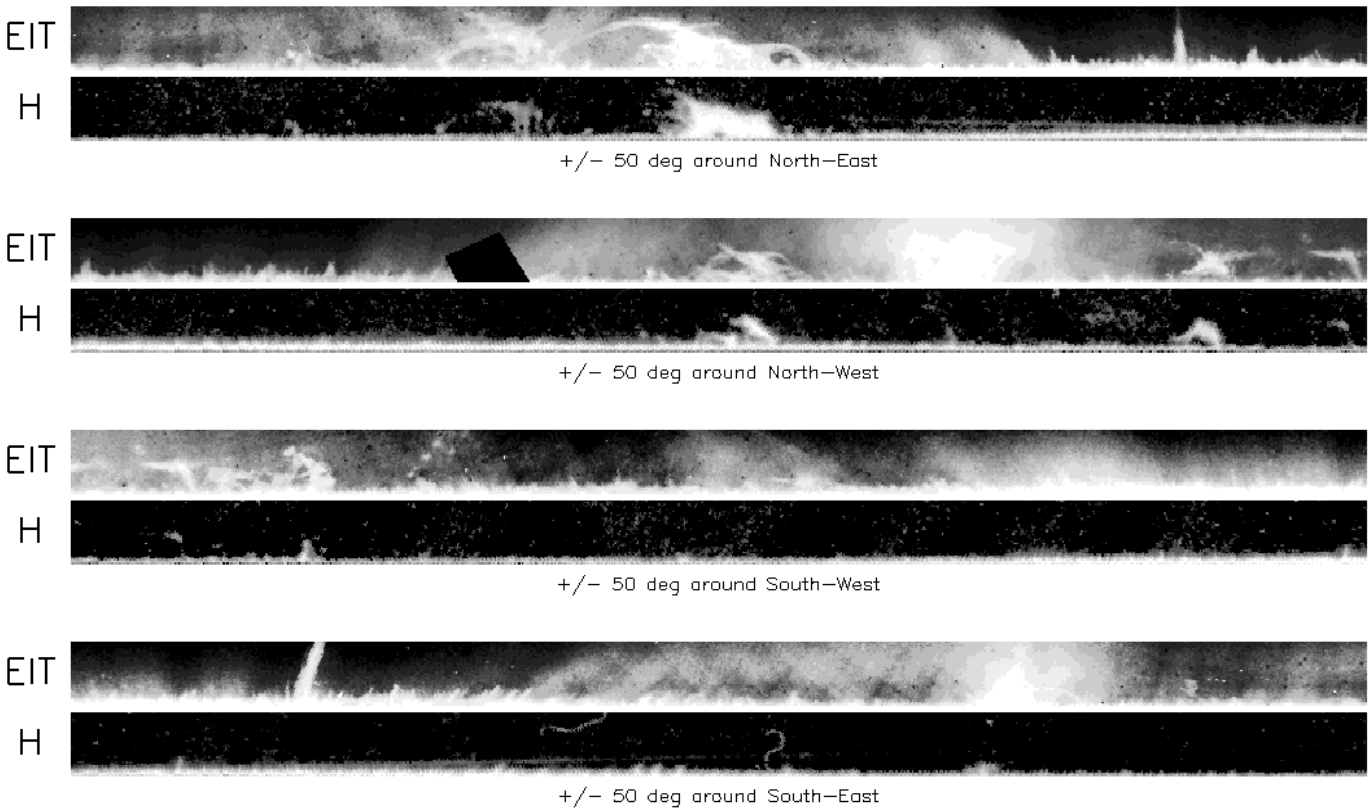

Fig. 1. Example of sub-frames near the poles and near the equator to show the limbs observed simultaneously with EIT using the HeII line at 304 Å and with the ground-based NSO/SP "one shot" coronograph at H_α with a 0.1 nm passband

steps was applied to corresponding image pairs. By this method, a pronounced maximum in the correlation was found (this procedure might require omitting, for example, the largest prominence that, because of its different morphologies in the two lines, could distort, or bias, the overall fit). It was found that an excellent overall correlation does exist between the full limb features in the two lines, although local details can appear quite different. Small features do not correlate, as indicated above.

2.3. The solar prolateness

This procedure then allowed an exact comparison between these space and ground-based images, and by extension the shape of the chromosphere of the Sun as observed in H_α and in HeII emission (see Fig. 1). We looked at the edges defined by a half-density inflection-point, which in turn has allowed a comparison of the polar and equatorial diameters for both wavelengths. Densities in images are directly related to the logarithmic values of intensities, as usual. Furthermore, the determination of the position of the limb is done using different lengths on each side of the poles or the equators in order to reduce the noise produced by variations due to small features. Taking into account distortion due to monochromatic dispersion in the Earth's atmosphere, it was found that the solar chromosphere as observed with a 0.1 nm FWHM Lyot filter centered on the H_α line is prolate to an extent of 2.2 ± 0.1 arcsec (over a solar diameter); this value is possibly a function of the phase of the solar activity cycle. The corresponding value estimated for the HeII emission is ~ 15 arcsec prolate. This latter result assumes negligible image distortion (see below, Sect. 3.2). We recall that by contrast, measurements of the photosphere report an oblateness of perhaps 10 milli-arcsec (Kuhn, 1997).

3. Improved analysis with the EIT images alone

These preliminary results showed an obvious prolateness of the solar chromosphere, for single measurements made in both H_α and HeII images. But a more systematic study is necessary, not only to obtain a more precise value of the prolateness, but also to look at the whole shape of the solar limb and its possible variations in time. This was done with the EIT images, now including all spectral-line channels and not only the 30.4 nm line.

3.1. Data processing

The EIT EUV imager (Delaboudinière et al., 1995) provides 1024×1024 pixels full-disk images in four wavelengths: 30.4 nm (HeII), 28.4 nm (FeXV), 19.5 nm (FeXII) and 17.1 nm (FeIX/FeX). We used all the images without data gaps on the solar limb available since the launch of SoHO. We defined the solar limb as the minimum of the radial gradient of intensity

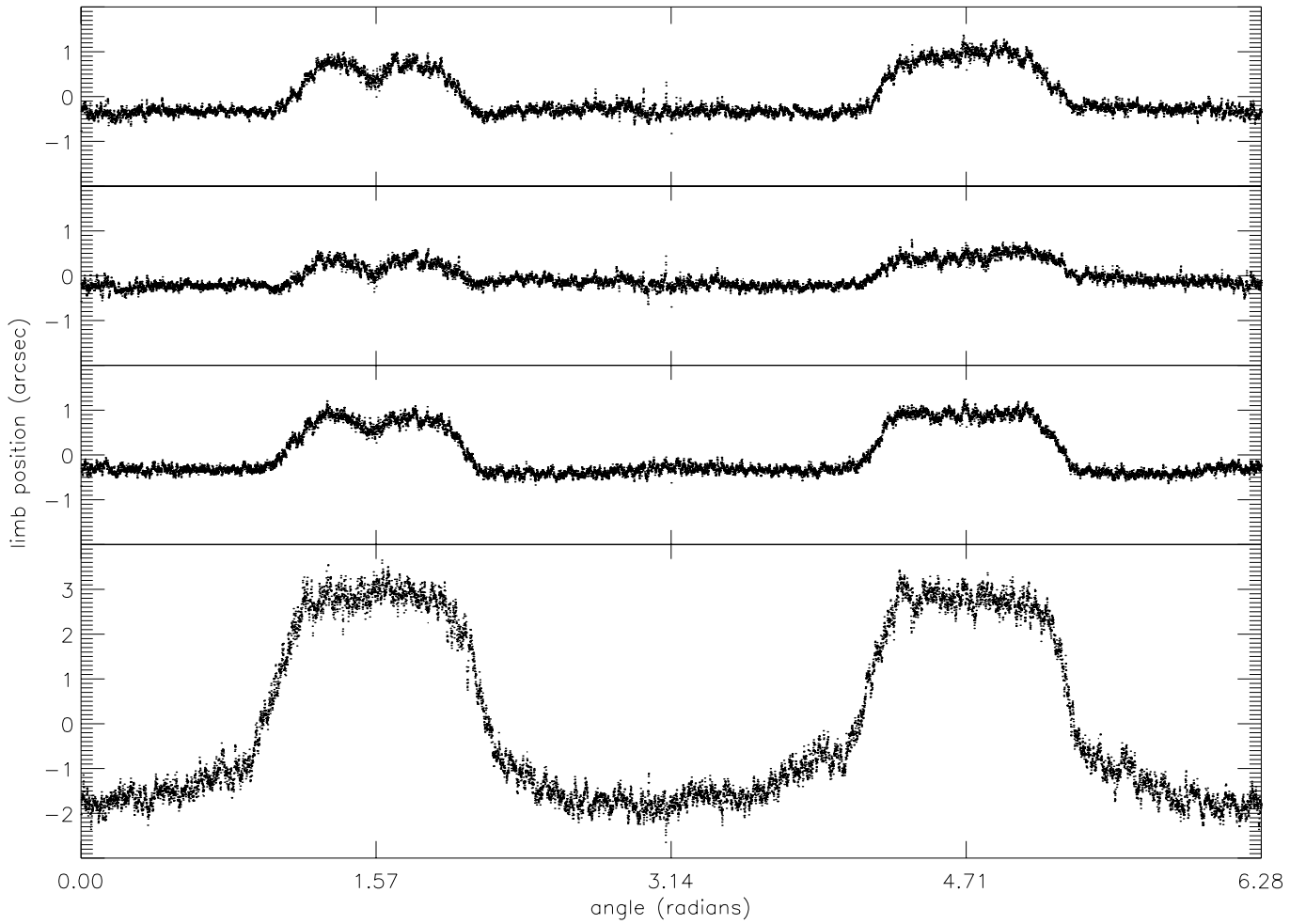

Fig. 2. Mean limb positions (over 400 images) relative to the best circular fit, for the four EIT channels. From top to bottom: 17.1 nm (FeIX/FeX), 19.5 nm (FeXII), 28.4 nm (FeXV), 30.4 nm (HeII)

outward the disk for the HeII line, and as the maximum toward the disk for the three iron lines. Assuming that the intensity is a strictly monotonic function of the solar radius around the limb, this definition is equivalent to looking at the inflexion point, but is less noisy for numerical processes. In order to find the limb automatically on each image, we developped an iterative routine. It starts using some initial sun-center coordinates, then it computes the maximum of the radial gradient along 10000 directions (using 3-points Lagrangian interpolation) and further fits the resulting profile with a circle. This allows the corrected coordinates to be obtained, wich then become the new initial ones, and so on until they are converging. With this method, we were sure to find the best circular fit for each image. The resulting four sets of profiles (one per wavelength) allowed us to compute the mean profiles over a two-years interval (Fig. 2).

3.2. Results and first comments

We notice on the four channels a rather circular shape at low latitudes (especially in the three iron lines), and two bumps over the poles, with a relatively sharp transition. We disregard the smallest features which are probably due to local defects on the CCD. The mean prolateness over a solar diameter is 10.4 ± 0.1 arcsec for HeII, 1.0 ± 0.1 arcsec for FeXII, and 2.1 ± 0.1 arcsec for FeIX/X and FeXV. Note that if we make the same measurements on log-scaled images as was done preliminary (see part 2.3), we find a prolateness of 14.0 arcsec, quite close to the first estimation. Using the images taken during different SoHO roll maneuvers, we verified that the observed prolateness is not an instrumental bias due to non square-shaped pixels. A temporal running mean shows that, in all wavelenghts, there were no significant variations of the prolateness during the last two years. To permit a better evaluation of the relative amplitudes of the prolateness compared to other sources of distorsion of the solar limb at large scale, Fig. 3 gives the amplitude spectra (FFT) for the dipole and quadrupole components, and higher orders. For the HeII limb data, the ratio of amplitudes of the dipolar to the quadrupolar component is more than 4. We did estimate the typical heights of formation, using images taken at the limb, in

Fig. 3. Amplitude spectrum of the solar limb for the four EIT channels. Solid: 30.4 nm, dotted: 28.4 nm, dashed: 19.5 nm, dash dots: 17.1 nm.

Table 1. prolateness (over a solar diameter) and estimated equatorial altitude of the limb above $\tau = 1$ for different lines

line	HeII	FeXV	FeXII	FeX	H_α
altitude (Mm)	5.5	2.5	2.5	2.5	4.0
ΔD (arcsec)	10.4	2.1	1.0	2.1	2.2

the spectral windows we used: H_α, HeII 30.4 nm and the coronal channels. Table 1 gives the results.

4. Discussions

The reason for a prolate chromosphere is not completly understood. However, since the chromosphere is a magnetically-dominated atmosphere, the distribution of the chromospheric plasma presumably relates to the predominantly radial direction of the field lines at the poles, especially around solar minimum, as proposed much earlier by A. H. Gabriel. The different scale heights for these two lines presumably results in the HeII emission "magnifying" the effect, as well as the effect of prolateness. For the moment, we have demonstrated tha H_α full-limb coronal images show a definite prolateness quite well, although coronal holes are not seen in H_α. We estimated the equatorial H_α limb to be at an average height of order of 4.0 Mm, in agreement with the classical work of Dunn, 1960, although this point needs further careful discussion. Using the same approximations, the HeII limb is estimated to be at 5.0 Mm in equatorial regions. In HeII, the prolateness is quite large. We are now looking at lower levels to check where the prolateness starts. As shown in Table 1, coronal data show a smaller prolateness, of order of $\Delta D/D = 0.5 \times 10^{-3}$, two times smaller than the H_α prolateness. However, the inner corona "limb" is also deeper; the VLA model puts the top of chromosphere at 2.1 Mm; then the corona penetrates in the transition region to the 2.5 Mm heights (see also Daw et al., 1995). Overall, the prolateness that we measure increases with the height above the classical chromosphere, see Table 1. To make the connexion with the high corona, recall that the solar corona is "flattened" equatorially; indeed, the heliosphere at solar minimum is made of two components, the fast wind and the helio-sheet and/or the slow wind. We speculate that the prolate chromosphere is linked closely with the origin of this behaviour, since it could produce the fast wind with an interplay between the dynamical pressure and the magnetic structure on a global scale.

References

Beckers, J.M., 1960, BAIN, XV, 497, 85
Daw A., DeLuca E., Golub L., 1995, ApJ 453, 929
Delannee C. et al., 1997, Proc. Fifth SOHO Workshop, ESA SP-404, 32
Delaboudinière J.P. et al., 1995, Solar Physics 162: 291–312
Dunn R.B., 1960, Ph. D. of Harvard University
Huber M.C. E. et al., 1974, ApJ, 194:L115–L118
Kuhn J.R., Bush R.I., Scheick, X. and Sherrer. P., 1998, Nature 392, 155
Moe O.K. et al., 1975, Solar Physics 40, 65–68
Secchi S.J., 1877, in: Le Soleil, Gauthier-Villars, p. 38
Rozelot J.P., Rösch J., 1996, C. R. Acad. Sci. Paris, t. 322, Série II *b*, p. 637–644
Withbroe G.L. et al., 1976, ApJ 203:528–532